

Electronic Supplementary Information (ESI) for:

Mitochondrion targeted Single-Layered Graphene Quantum Dots with Dual Recognition Sites for ATP Imaging in Living Cells

*Jia Hui Liu, ^a Rong Sheng Li, ^a Binfang Yuan, ^c Wang jian, ^{a, *} Yuan Fang Li ^b and Cheng Zhi Huang ^{a, b, *}*

^a Key Laboratory of Luminescent and Real-Time Analytical Chemistry (Southwest University), Ministry of Education, College of Pharmaceutical Sciences, Southwest University, Chongqing 400716, China.

^b Chongqing Key Laboratory of Biomedical Analysis (Southwest University), Chongqing Science & Technology Commission, College of Chemistry and Chemical Engineering, Southwest University, Chongqing 400715, China.

^c School of Chemistry and Chemical Engineering, Yangtze Normal University, Chongqing 408100, China

*Correspondence and requests for materials should be addressed to W, J. or H, C. (email: chengzhi@swu.edu.cn, wj123456@swu.edu.cn)

Experimental section

Synthesis of the s-GQDs

The s-GQDs were prepared through a simple one-step hydrothermal synthesis route. Briefly, 0.5 g PEI was dissolved in 10 ml anhydrous ethanol, and then added 0.1 g PTCA to a 25 ml Teflon-lined stainless steel autoclave. After fully mixing, the mixture was incubated at 180 °C for 24 h in a temperature well-controlled oven. With the reaction completion, the autoclave was cooled down to room temperature naturally, and the reactive solution was then centrifuged at 8000 rpm for 10 min to remove the large deposit. The resulting supernatant was concentrated and then purified through a membrane (3500 MWCO) over 48 h to discard the residual reagents. Finally, the obtained s-GQDs were frozen at -20 °C and dried under vacuum. Other GQDs were synthesized by changing the ratios of PTCA and PEI.

Interaction of nucleoside polyphosphates with s-GQDs

All stock solutions of polyphosphates were first prepared and then diluted into a series of concentrations with deionized water. 0.1 ml of s-GQDs solution ($5\mu\text{g mL}^{-1}$) was mixed with 0.1 ml polyphosphates with various concentrations, and then diluted to 1.0 ml with sodium acetate-acetic acid buffer (pH 5.4) through mixing to form a homogeneous solution. 10 min later, the prepared solutions were then transferred to measure PL emission features at room temperature.

Cellular Toxicity Test

HeLa cells were used to evaluate the cytotoxicity of the s-GQDs through the conventional Cell Counting Kit-8 (CCK-8) method. In brief, 100 μL of 1.0×10^5 cells per mL of HeLa cells was added to each well of a 96 well plate, in which 90 μL Roswell Park Memorial Institute 1640 medium (RPMI 1640) supplemented with 2% fetal bovine serum were contained. Then, the cells were cultured for 24 h in an incubator (37 °C, 5% CO_2), and for another 24 h, 48 h, or 72 h of being cultured with the 90 μL of Roswell Park Memorial Institute 1640 medium (RPMI 1640) containing 10 μL of the s-GQDs with various concentrations (0, 10, 20, 40, 60, 80, 100 $\mu\text{g mL}^{-1}$). After incubation, removing the culture medium, the cells were washed with PBS buffer for three times, and then 10 μL of Cell Counting Kit-8 (CCK-8) solution was added to each cell well, in which 90 μL RPMI 1640 was contained. After another incubation of 0.5 h (the solution of well became yellow), the optical density (OD) of the mixture was recorded with Micro plate Reader Model (for three times). The values of cell viability were calculated based on the following equation:

$$\text{Cell viability [\%]} = (\text{OD treated}/\text{OD control}) \times 100$$

Wherein OD control was obtained in the absence of s-GQDs, and OD treated was obtained in the presence of s-GQDs.

Imaging of mitochondrial ATP with s-GQDs

Firstly, the HeLa cells in RPMI 1640 supplemented with 10% fetal bovine serum were added to two petri dishes (300 μL per dish). The cells were cultured first for 24 h in an incubator (37 °C, 5% CO_2), and for another 24 h after replacing the medium with 270 μL of RPMI 1640 and 30 μL s-GQDs (at the concentration of 100 $\mu\text{g mL}^{-1}$). Afterwards, discarding the culture medium, each dish was washed with PBS buffer for three times, the s-GQDs-loaded cells were incubated with 100 μL of ATP (1 mM) for 5 min. Finally, the samples were imaged with laser confocal fluorescence microscopy (LCFM) and the images were analyzed using Image-Pro Plus software. **Co-staining imaging in living cells**

To investigate the co-localization imaging of HeLa cells staining with Mito-Tracker Green, the HeLa cells were cultured in RPMI 1640 (Hyclone) media supplemented with 10 % foetal bovine serum (FBS, Hyclone), 100 U mL^{-1} penicillin G and 100 $\mu\text{g mL}^{-1}$ streptomycin sulphate in a CO_2 incubator at 37 °C. One day prior the adding of s-GQDs, the cells were seeded on 35 mm glass-bottom dishes (NEST. Corp.) To investigate whether s-GQDs could stain the mitochondria, Tracker Green (Beyotime Biotechnology) was used to co-stain the mitochondria of HeLa cells. The cells were incubated with s-GQDs (100 $\mu\text{g mL}^{-1}$) for 2 h, and then Mito-Tracker Green (100 nM) was added. The cells were incubated for 20 min in a CO_2 incubator at 37 °C after the adding of Mito-Tracker Green. The cells were then washed and finally observed under a confocal microscope.

Imaging the ATP fluctuation in mitochondrion

In order to test the ATP-dependent fluctuations, 2.0 mM sodium azide or 5.0 mM Ca^{2+} were added in the cell culture for 2 h in a CO_2 incubator at 37 °C. Then s-GQDs were added and incubated for another 2 h. After washing three times with phosphate buffered saline (PBS), the cells were observed under a confocal microscope.

Flow Cytometry Analysis

Flow cytometry analysis was performed on a FACScan cytometer to demonstrate the the PL intensities of s-GQDs in the cells with different treatments. Herein, we treated HeLa cells with Ca^{2+} and sodium azide to regulate intracellular ATP generation. Briefly, 2.0 mM sodium azide and 5.0 mM Ca^{2+} were added in the cell culture for 2 h in a CO_2 incubator at 37 °C, respectively. Then s-GQDs were added and incubated for another 2 h. After washing three

times with phosphate buffered saline (PBS), Cells were subjected to flow cytometry analysis by counting 10,000 events.

Materials and Apparatus

Adenosine 5'-triphosphate sodium salt (ATP), adenosine 5'-diphosphate sodium salt (ADP), adenosine 5' monophosphate sodium salt (AMP), guanosine 5'-triphosphate sodium salt hydrate (GTP), guanosine 5'-diphosphate sodium salt hydrate (GDP), guanosine 5'-monophosphate sodium salt hydrate (GMP), cytidine 5'-triphosphate sodium salt hydrate (CTP), uridine 5'-triphosphate sodium salt hydrate (UTP) were all bought from Sigma-Aldrich (St Louis, MO) and stored under specified conditions. 3, 4, 9, 10-Perylenetetracarboxylic acid anhydride (PTCA) and polyethylenimine (PEI, Mw=1800) were purchased from Aladdin Chemistry Co. Ltd. (Shanghai, China). Anhydrous ethanol, acetic acid, sodium acetate, sodium phosphate (Pi) and sodium pyrophosphate (PPi) were purchased from East Sichuan Chemistry of Chongqing Co. Ltd. (Chongqing, China). Beta 1 Sodium Potassium ATPase (Specific activity is > 3,000 pmol/min/μg, and is defined as the amount of enzyme that hydrolyze 1.0 pmole of Adenosine 5-triphosphate to phosphate per minute per minute at pH 7.5 at 25°C.) was purchased from Abcam. ELISA kits of Alpha-1-Acid Glycoprotein (α 1-AGP), Mucin 2 (MUC 2), Vascular Endothelial Growth Factor C (VEGF-C), Basic Fibroblast Growth Factor (FGF 2), Tumor Protein p53 (TP53), and Caspase 3 (CASP 3) were purchased from Abcam. All chemicals were of analytic al grade and were used without further purification. Sodium acetate-acetic acid buffer solution was used to control the acidity of the solutions. All solutions of nucleotide were stored in 4°C, and used up within a month. Millipore purified water (18.2 MΩ) was used throughout.

Absorption and fluorescence spectra were recorded by the UV-3600 spectrophotometer () and F-2500 fluorescence spectrophotometer (Hitachi Ltd, Tokyo, Japan), respectively. High-resolution TEM (HRTEM) images and fast Fourier transform (FFT) spot diagrams of the QDs were recorded with a high resolution transmission electron microscope (Tecnai G2 F20S-TWIN, FEI Company, USA). Atomic force microscopy (AFM) images were captured on a Dimension Icon Scan Asyst atomic force microscope (Bruker Co.). The Raman spectrum of the as-obtained sample on an Ag substrate was recorded on a LabRAM HR800 Laser confocal Raman spectrometer (Horiba Jobin Yvon Inc., France) at ambient temperature (about 25°C). Elemental and functional groups analysis was performed on an ESCALAB 250 X-ray photoelectron spectrometer (USA) and a FTIR-8400S Fourier transform infrared spectrometer (Kyoto, Japan), respectively. The fluorescence life time was obtained with an FL-TCSPC fluorescence spectrophotometer (Horiba Jobin

Yvon Inc., France). Zeta potentials and hydrodynamic size were measured by dynamic laser light scattering (ZEN3600, Malvern). Cellular imaging was conducted through the Olympus DSU live-cell confocal microscope (Tokyo, Japan) system and Zeiss LSM 800. FACScan cytometer (Becton Dickinson Immunocytometry Systems, San Jose, CA, USA) was used to analysis the PL intensities of s-GQDs in the cells with different treatments.

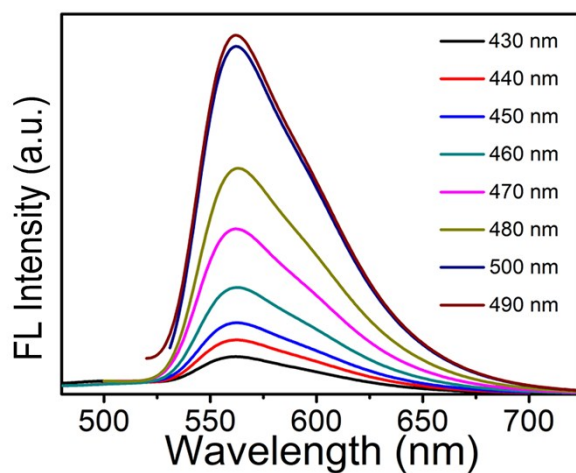


Figure S1 Emission spectra of s-GQDs at different excitation wavelengths (λ_{ex} =430, 440, 450, 460, 470, 480, 490, 500 nm).

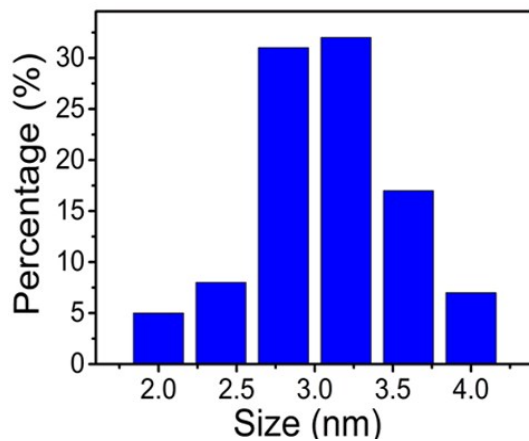


Figure S2 Particle size distribution of s-GQDs (50 particles were selected for statistical analysis).

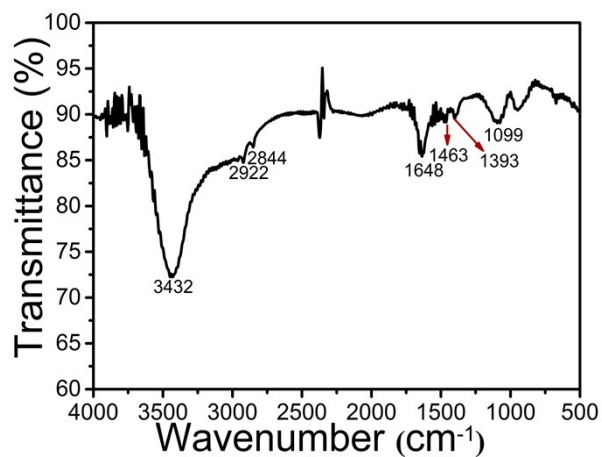


Figure S3 Infrared spectrum of s-GQDs. The absorption bands of the FTIR spectrum indicates the existence of amine (3432 cm^{-1}), amide carbonyl (1648 cm^{-1}), C=C (1463 cm^{-1}), C-N (1393 cm^{-1}) and C-O (1099 cm^{-1}) functional groups or chemical bonds.¹⁻³

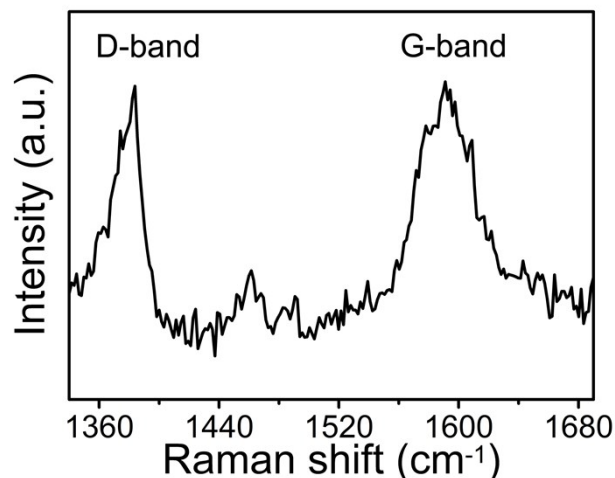


Figure S4 Raman spectrum of s-GQDs. The Raman spectrum illustrates two prominent peaks at approximately 1383 cm^{-1} and 1591 cm^{-1} , which are attributed to the disordered D-band (sp^3 -hybridized) and crystalline G-band (sp^2 -hybridized), respectively.⁴

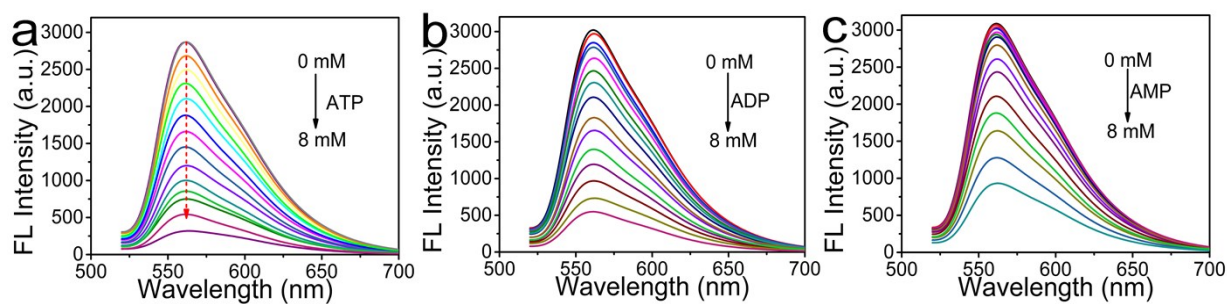


Figure S5 Fluorescence emission spectra of s-GQDs ($100\text{ }\mu\text{g mL}^{-1}$) ($\lambda_{\text{ex}}=490\text{ nm}$) with addition of (a) ATP, (b) ADP, (c) AMP with increasing concentration (0, 0.1, 0.2, 0.4, 0.6, 0.8, 1.0, 1.5, 2.0, 3.0, 4.0, 5.0, 6.0, 7.0 and 8.0 mM) in 0.2 M acetic acid-sodium acetate buffer solution (pH 5.4).

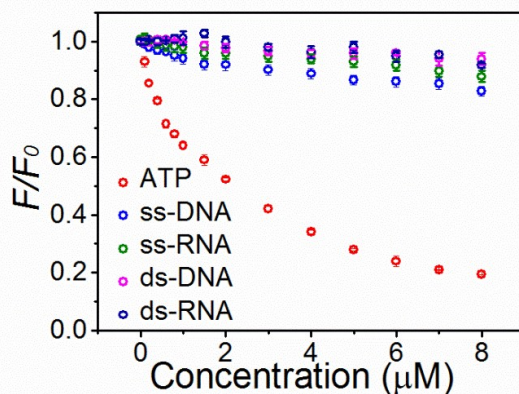


Figure S6 Fluorescence response curve of s-GQDs ($5 \mu\text{g mL}^{-1}$) with ATP, RNA and DNA of increasing concentrations (0, 0.1, 0.2, 0.4, 0.6, 0.8, 1.0, 1.5, 2.0, 3.0, 4.0, 5.0, 6.0, 7.0 and $8.0 \mu\text{M}$), (37°C , Tris-HCl pH 7.0).

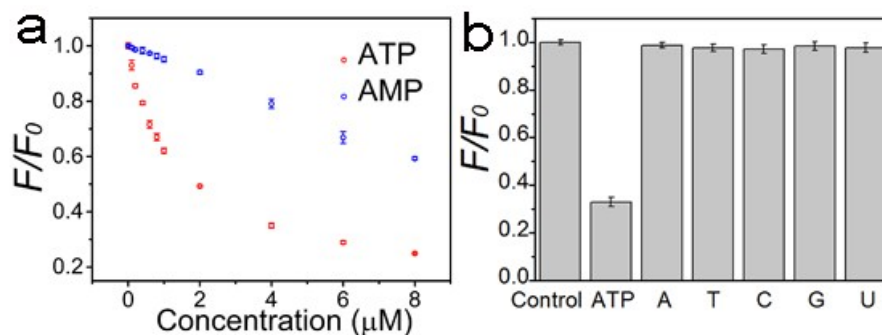


Figure S7 The interaction of s-GQDs ($5 \mu\text{g mL}^{-1}$) with nucleobases and adenine nucleotides. (a) Fluorescence response value of s-GQDs with ATP ($4 \mu\text{M}$) and four nucleobases: adenine (A), thymine (T), cytosine (C), guanine (G) and uracil (U), ($4 \mu\text{M}$, 37°C , Tris-HCl pH 7.0). (b) Fluorescence response curve of s-GQDs ($5 \mu\text{g mL}^{-1}$) with ATP and AMP of increasing concentrations (0, 0.1, 0.2, 0.4, 0.6, 0.8, 1.0, 2.0, 4.0, 6.0 and $8.0 \mu\text{M}$), (37°C , Tris-HCl pH 7.0). Error bars represent standard deviations from three replicate experiments.

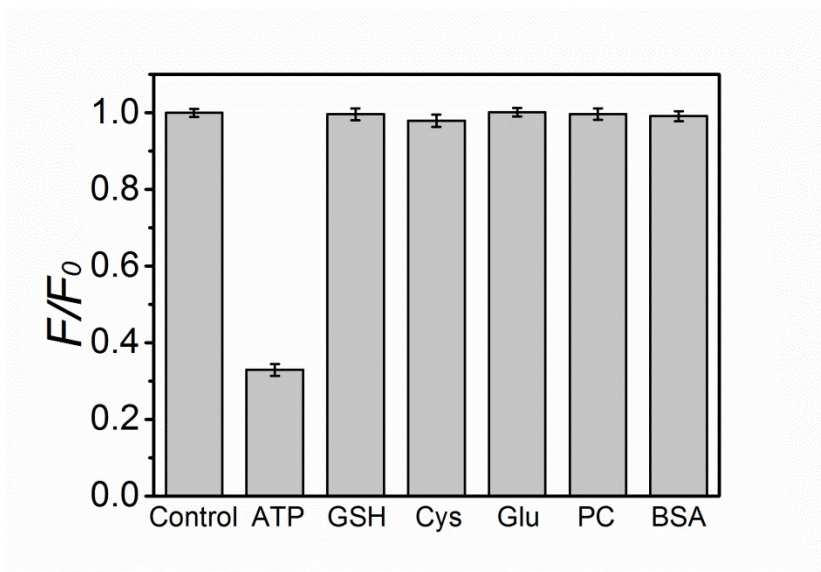


Figure S8 The interaction of s-GQDs ($5 \mu\text{g mL}^{-1}$) with other molecules: glutathione (GSH), cysteine (Cys), glucose (Glu), phosphatidylcholine (PC) and bovine serum albumin (BSA) ($4 \mu\text{M}$, 37°C , Tris-HCl pH 7.0). Error bars represent standard deviations from three replicate experiments.

Notes:

To investigate the interaction between s-GQDs and other molecules with big π rings such as DNA and RNA, we did a large amount of experiments.

First, a random single strand DNA (ssDNA) and a random single strand RNA (ssRNA) of 24 bases in length with different concentrations were added into the $5 \mu\text{g mL}^{-1}$ s-GQD solutions (37°C , Tris-HCl pH 7.0). As shown in Figure S6, s-GQDs have weak binding ability to DNA ($0\text{-}8.0 \mu\text{M}$) and RNA ($0\text{-}8.0 \mu\text{M}$) compared with ATP ($0\text{-}8.0 \mu\text{M}$), as evidenced by no significant changes in fluorescence intensity of s-GQD in DNA and RNA solutions. Similarly, s-GQDs have also weak binding ability to the double strand DNA (dsDNA) and double strand RNA (dsRNA). The reason of low response of s-GQDs to DNA and RNA may as follows:

(1) There is only one phosphate in each monomeric nucleotide units in DNA strands. DNA is composed of nucleotides. Each nucleotide is composed of one of four nucleobases, a sugar called deoxyribose, and a phosphate group. The structure of single nucleotide is similar with AMP because there is only one phosphate in each nucleotide. Similar with the low affinity of s-GQDs with AMP compared with ATP (Figure S7a), the s-GQDs may have a low affinity with DNA and RNA compared with ATP.

(2) There are two covalent bonds on phosphate between two nucleosides. The nucleotides in DNA and RNA are joined to one another in a chain by covalent bonds between the sugar of one nucleotide and the phosphate of the next. The phosphate between two nucleosides has a low ionization ability because the

two covalent bonds on phosphate. However, the triphosphate in ATP has a high ionization capacity. Stronger negative charge is better for the interaction between s-GQDs and ATP.

(3) There is no response of s-GQDs for nucleobases such as adenine (A), thymine (T), cytosine (C), guanine (G) and uracil (U). We have studied the interaction of s-GQDs ($5 \mu\text{g mL}^{-1}$) with nucleobases ($4 \mu\text{M}$) and adenine nucleotides ($4 \mu\text{M}$) (Figure S7b). The fluorescence of s-GQDs would not quench in five kinds of nucleobase solutions. The results may attribute to the weak positive charge of nucleobases.

Random single strand DNA sequence:

5'- AGT CAG TGT GCA CGA TCT CTA GCA -3'

Complementary sequence of random single strand DNA:

5'- TGC TAG AGA TCG TGC ACA CTC ACT -3'

Random single strand RNA sequence:

5'- AGU CAG UGU GCA CGA UCU CUA GCA -3'

Complementary sequence of random single strand RNA:

5'- UGC UAG AGA UCG UGC ACA CUC ACU -3'

Second, the s-GQD can selectively accumulate in mitochondrion. The average concentration of ATP in mitochondrion is about 1–5 mM (*Anal. Chem.*, 2017, **89**, 1749-1756; *J. Am. Chem. Soc.*, 2017, **139**, 5877-5882). The concentration of mitochondrial DNA AND mitochondrial RNA are much lower than 1 mM (*Nucleic Acids Res.* 2002, **30**: e68; *Science.* 2017, **287**: 2017-2019). Owing to the high concentration of ATP and high response ability of s-GQDs for ATP, the fluorescence change of s-GQD should attributed to the fluctuation of ATP in living cells.

Taking together, we may draw the conclusion that the fluorescence change of s-GQD are caused by the fluctuation of ATP in mitochondrion of living cells. We have added this part of work in the revised manuscript and revised supporting information.

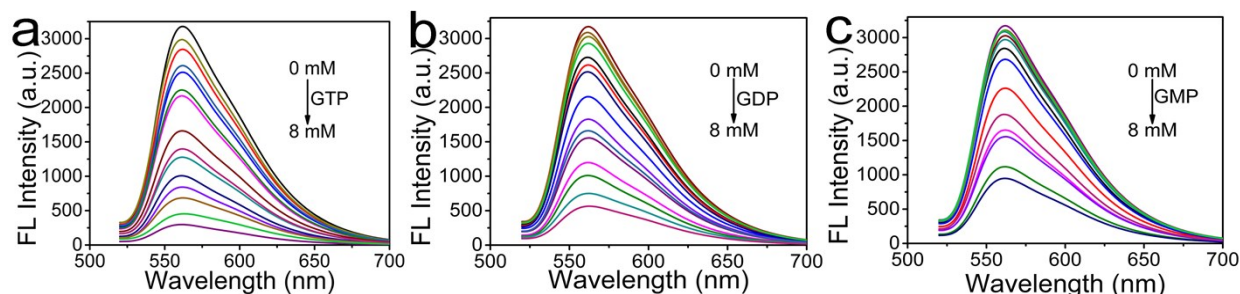


Figure S9 Fluorescence emission spectra of s-GQDs ($100 \mu\text{g mL}^{-1}$) ($\lambda_{\text{ex}}=490 \text{ nm}$) with addition of (a) GTP, (b) GDP, (c) GMP with increasing concentration (0, 0.1, 0.2, 0.4, 0.6, 0.8, 1.0, 1.5, 2.0, 3.0, 4.0, 5.0, 6.0, 7.0 and 8.0 mM) in 0.2 M acetic acid-sodium acetate buffer solution (pH 5.4).

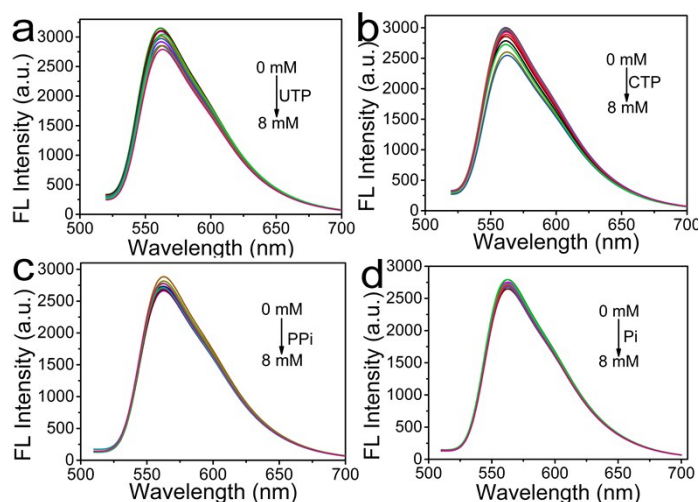


Figure S10 Fluorescence emission spectra of s-GQDs ($100 \mu\text{g mL}^{-1}$) ($\lambda_{\text{ex}}=490 \text{ nm}$) with addition of (a) UTP, (b) CTP, (c) Pi, (d) PPi with increasing concentration (0, 0.1, 0.2, 0.4, 0.6, 0.8, 1.0, 1.5, 2.0, 3.0, 4.0, 5.0, 6.0, 7.0 and 8.0 mM) in 0.2 M acetic acid-sodium acetate buffer solution (pH 5.4).

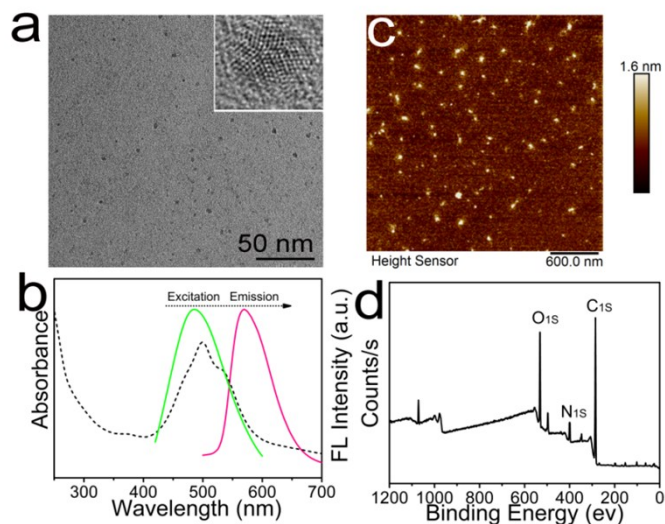


Figure S11 Optical and morphology properties of GQDs (1:1; prepared by 0.1 g PTCDA and 0.1 g PEI). (a) TEM image of the prepared GQDs. Inset: HRTEM image of single GQDs particle. (b) AFM image of GQDs. (c) Emission spectrum (pink) was obtained under maximum excitation at 490 nm, and the excitation spectrum (green) was obtained at the maximum emission wavelength at 562 nm. The black dotted line curve shows the absorption spectrum of the prepared GQDs. (d) Full XPS spectrum of GQDs.

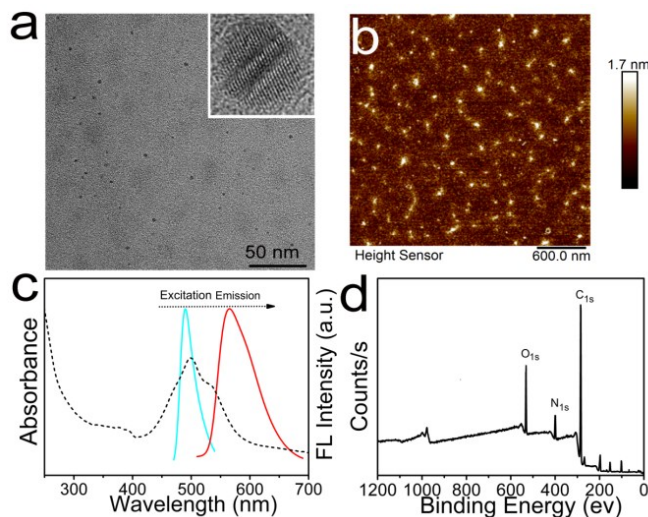


Figure S12 Optical and morphology properties of GQDs (1:3; prepared by 0.1 g PTCDA and 0.3 g PEI). (a) TEM image of the prepared GQDs. Inset: HRTEM image of single GQDs particle. (b) AFM image of GQDs. (c) Emission spectrum (red) was obtained under maximum excitation at 490 nm, and the excitation spectrum (cyan) was obtained at the maximum emission wavelength at 562 nm. The black dotted line curve shows the absorption spectrum of the prepared GQDs. (d) Full XPS spectrum of GQDs.

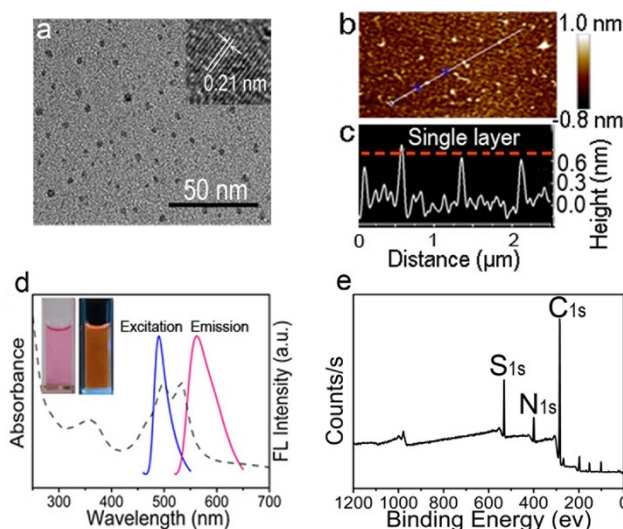


Figure S13 Optical and morphology properties of GQDs (1:5; prepared by 0.1 g PTCDA and 0.5 g PEI). (a) TEM image of the prepared GQDs. Inset: HRTEM image of single GQDs particle. (b-c) AFM image of GQDs. (d) Emission spectrum (pink) was obtained under maximum excitation at 490 nm, and the excitation spectrum (blue) was obtained at the maximum emission wavelength at 562 nm. The black dotted line curve shows the absorption spectrum of the prepared GQDs. (e) Full XPS spectrum of GQDs.

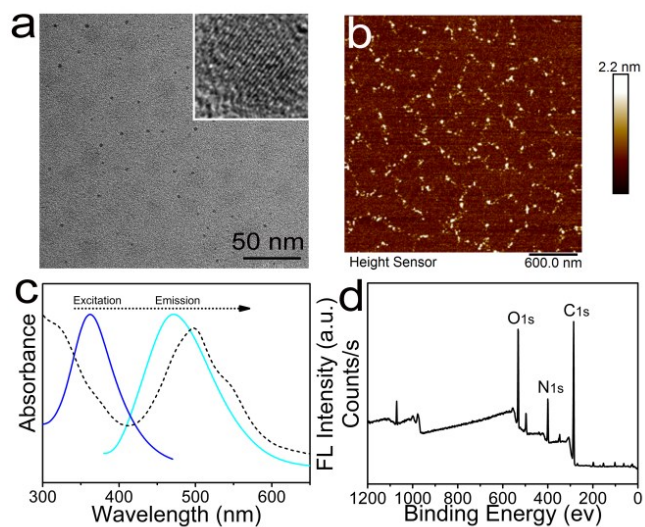


Figure S14 Optical and morphology properties of GQDs (1:10; prepared by 0.1 g PTCDA and 1.0 g PEI). (a) TEM image of the prepared GQDs. Inset: HRTEM image of single GQDs particle. (b) AFM image of GQDs. (c) Emission spectrum (cyan) was obtained under maximum excitation at 370 nm, and the excitation spectrum (blue) was obtained at the maximum emission wavelength at 475 nm. The black dotted line curve shows the absorption spectrum of the prepared GQDs. (d) Full XPS spectrum of GQDs.

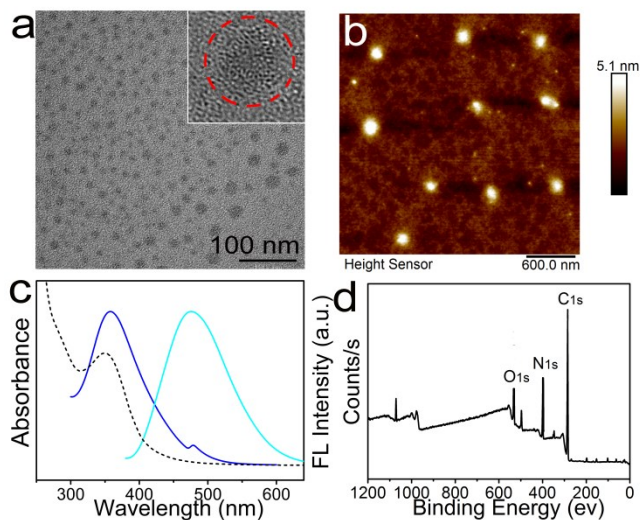


Figure S15 Optical and morphology properties of GQDs (0:5; prepared by 0.5 g PEI). (a) TEM image of the prepared GQDs. Inset: HRTEM image of single GQDs particle. (b) AFM image of GQDs. (c) Emission spectrum (cyan) was obtained under maximum excitation at 365 nm, and the excitation spectrum (blue) was obtained at the maximum emission wavelength at 485 nm. The black dotted line curve shows the absorption spectrum of the prepared GQDs. (d) Full XPS spectrum of GQDs.

Table S1 The elementary composition of different prepared GQDs.

Sample	C%	N%	O%
GQDs (1:1)	83.58	2.80	13.56
GQDs (1:3)	81.50	5.66	17.84
GQDs (1:5)	80.08	7.50	12.42
GQDs (1:10)	65.59	14.21	20.20
GQDs (0:5)	64.41	24.78	10.81

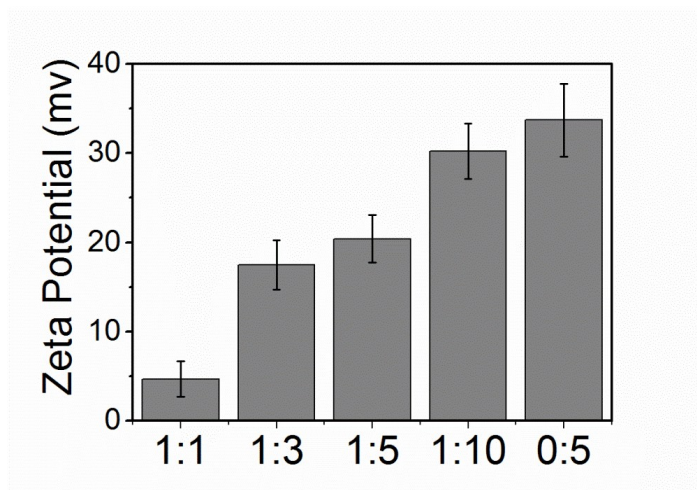


Figure S16 The zeta potential of different prepared GQDs (measured at 25 °C).

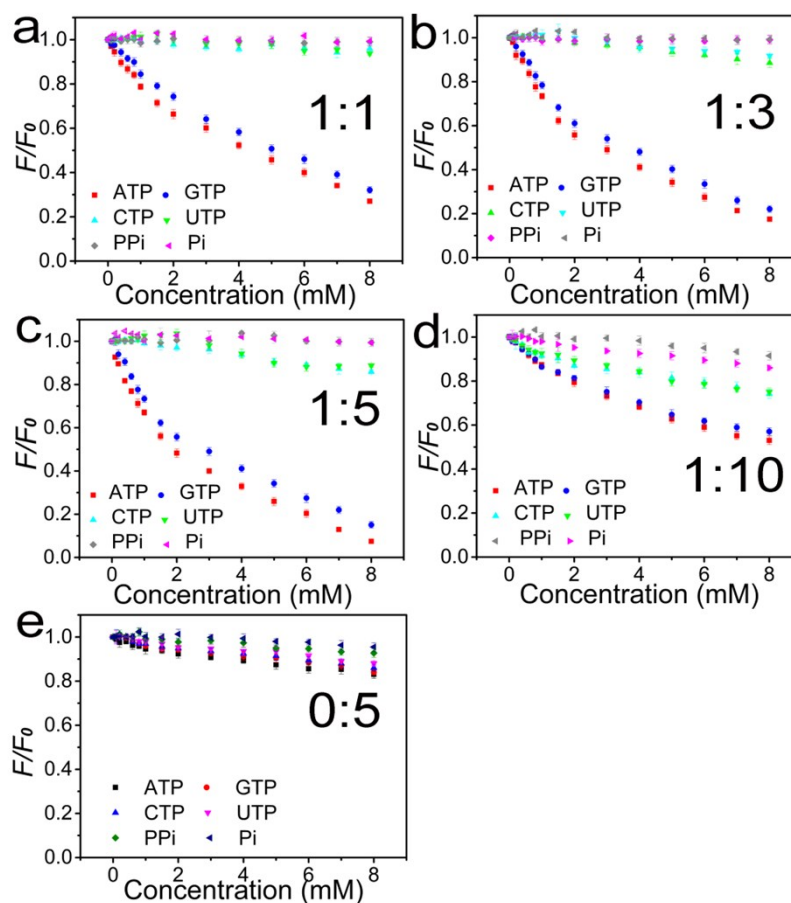


Figure S17 The interaction of different GQDs (prepared by different ratio of PTCDA and PEI, 100 $\mu\text{g mL}^{-1}$) with polyphosphates. GQDs were prepared by 0.1 g PTCDA + 0.1 g PEI (1:1) (a), 0.1 g PTCDA + 0.3 g PEI (1:3) (b), 0.1 g PTCDA + 0.5 g PEI (1:5) (c), 0.1 g PTCDA + 1.0 g PEI (1:10) (d), and 0.5 g PEI (e). (a-e) Fluorescence response curve of GQDs with different polyphosphates of increasing concentrations (0, 0.1, 0.2, 0.4, 0.6, 0.8, 1.0, 1.5, 2.0, 3.0, 4.0, 5.0,

6.0, 7.0 and 8.0 mM). F_0 is the fluorescence emission intensity in the absence of polyphosphates and F is the fluorescence emission intensity in the presence of different concentrations of polyphosphates. All the detection experiments have been carried out three times for RSD calculation.

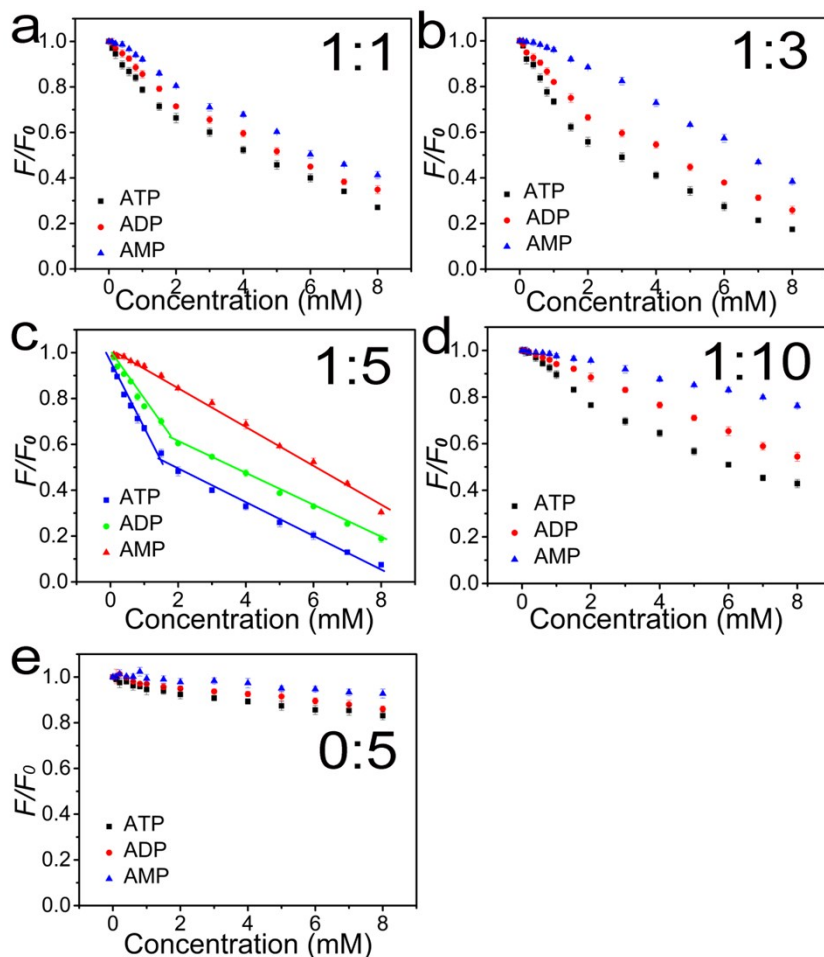


Figure S18 Fluorescence response curves of different GQDs (prepared by different ratio of PTCDA and PEI, 100 $\mu\text{g mL}^{-1}$) with adenine nucleotides. GQDs were prepared by 0.1 g PTCDA + 0.1 g PEI (1:1) (a), 0.1 g PTCDA + 0.3 g PEI (1:3) (b), 0.1 g PTCDA + 0.5 g PEI (1:5) (c), 0.1 g PTCDA + 1.0 g PEI (1:10) (d), and 0.5 g PEI (e). (a-e) Fluorescence response curve of GQDs with different adenine nucleotides of increasing concentrations (0, 0.1, 0.2, 0.4, 0.6, 0.8, 1.0, 1.5, 2.0, 3.0, 4.0, 5.0, 6.0, 7.0 and 8.0 mM). F_0 is the fluorescence emission intensity in the absence of polyphosphates and F is the fluorescence emission intensity in the presence of different concentrations of polyphosphates. All the detection experiments have been carried out three times for RSD calculation.

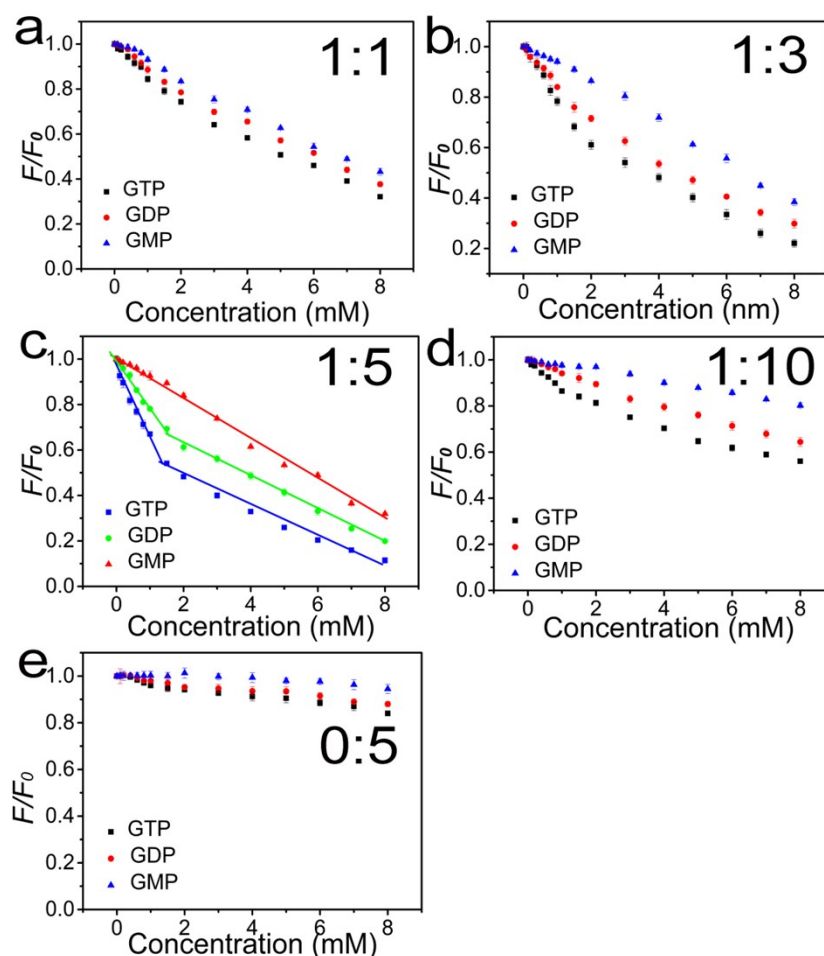


Figure S19 Fluorescence response curves of different GQDs (prepared by different ratio of PTCDA and PEI, 100 $\mu\text{g mL}^{-1}$) with guanine nucleotides. GQDs were prepared by 0.1 g PTCDA + 0.1 g PEI (1:1) (a), 0.1 g PTCDA + 0.3 g PEI (1:3) (b), 0.1 g PTCDA + 0.5 g PEI (1:5) (c), 0.1 g PTCDA + 1.0 g PEI (1:10) (d), and 0.5 g PEI (e). (a-e) Fluorescence response curve of CDs with different guanine nucleotides of increasing concentrations (0, 0.1, 0.2, 0.4, 0.6, 0.8, 1.0, 1.5, 2.0, 3.0, 4.0, 5.0, 6.0, 7.0 and 8.0 mM). F_0 is the fluorescence emission intensity in the absence of polyphosphates and F is the fluorescence emission intensity in the presence of different concentrations of polyphosphates. All the detection experiments have been carried out three times for RSD calculation.

Notes:

To investigate the sensing mechanism of our proposition of the interaction between s-GQDs and different nucleotides, five ratios of PTCDA and PEI were used to prepare s-GQDs: 1:0 (0.1 g PTCDA), 1:1 (0.1 g PTCDA, 0.1 g PEI), 1:3 (0.1 g PTCDA: 0.3 g PEI), 1:10 (0.1 g PTCDA: 1.0 g PEI) and 0:5 (0.5 g PEI), respectively. Among them, 1:1, 1:3, 1:10 and 0:5 can form GQDs while 1:0 could not form GQDs.

First, we investigated the structure and spectrum of these prepared GQDs (Figures S11-S15). The positive charge on the surface of GQDs would increase and the conjugated aromatic structure in the core of GQDs would decrease with the increasing of the PEI ratio in precursors. (Figure S16 and Table S1)

Second, we investigated the interaction of these prepared GQDs with different nucleotides and polyphosphates. All GQDs prepared by different ratio have no response to isolated nucleosides (A, T, C, G, A, and U), phosphate (Pi) and pyrophosphate (PPi). Furthermore, the GQDs prepared by pure PEI which has no large π systems show no response to nucleotides, nucleosides, phosphoric acid, and triphosphoric acid (Figures S17e, S18e, and S19e). The results show the importance of the concurrent of large π systems and positive charge for the sensing of nucleotides.

Third, different GQDs present different response to nucleotides which contain both nucleosides and triphosphate. On the one hand, GQDs with high ratio of PEI present increasing responses to weak negative charged ADP and AMP (Figures S17a-d, S18a-d, and S19a-d), which can attribute to the increased electrostatic interaction between positive charge GQDs and nucleotides. On the other hand, high ratio of PEI (1:10 ratio of precursors) presents bad selectivity for nucleotides and polyphosphates (Figures S17d, S18d, and S19d). The bad selectivity should be attributed to the decreased large π systems in GQDs (1:10). Importantly, a proper ratio of PTCDA and PEI (1:5, Figures S17c, S18c, and S19c) has good response to ATP/GTP, while show none response to other phosphates, such as CTP, UTP, Pi or PPi. The results indicate the importance of the concurrent effect of the dual recognition sites of π - π stacking and electrostatic interactions.

According to the experimental results above, we could draw the conclusion that the selectivity for purines and differentiation of tri-, di- and mono-phosphates is the concurrent effect of π -conjugated single layer plane and positively-charged amino groups. We have added this part of work in the revised manuscript and revised supporting information.

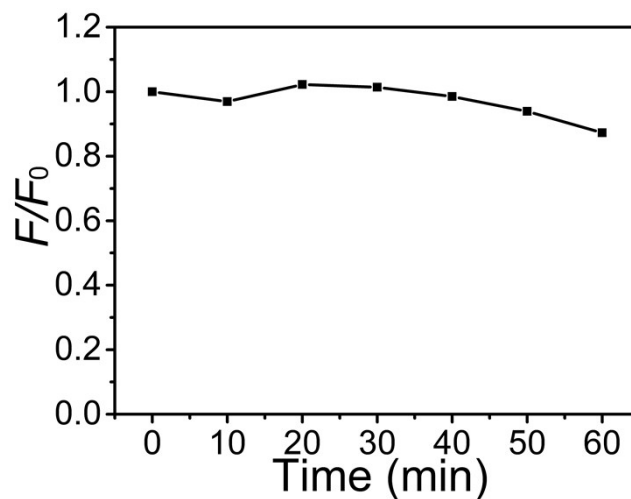


Figure S20 The s-GQDs are photo-stable under continuous irradiation of Xe lamp (spectral output: 320 nm-2500 nm, $U=14$ V, $A=12$ A) for 60 min. (F_0 and F correspond to the fluorescence intensity of s-GQDs at 562 nm in the absence and presence of irradiation, respectively).

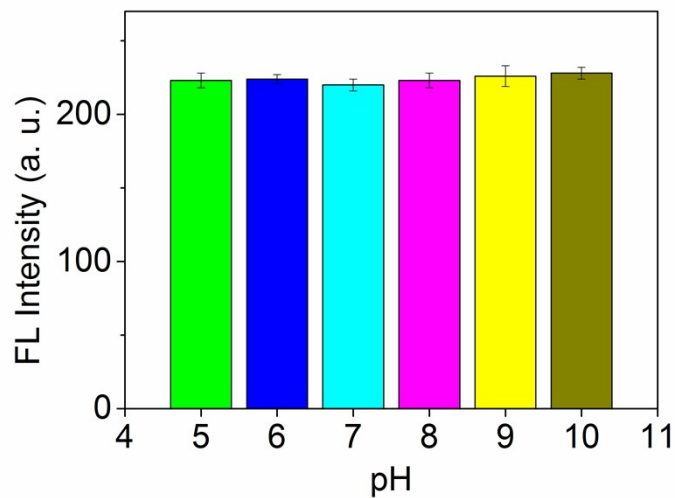


Figure S21 The s-GQDs are stable under pH values ranging from 5 to 10, as verified by the minimal change of fluorescence intensity as pH varies.

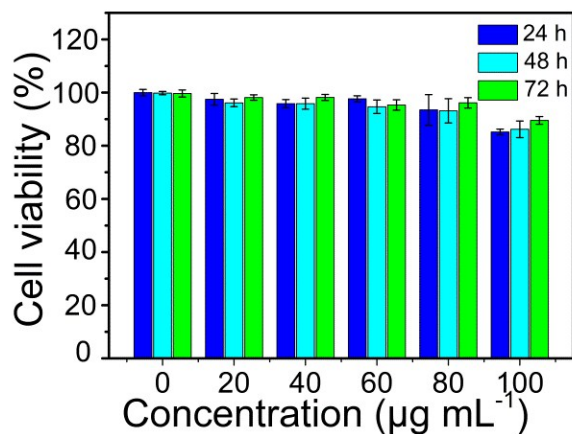


Figure S22 Cell viability assays of the cells treated with different concentrations (0, 20, 40, 60, 80 and 100 µg mL⁻¹) of s-GQDs at 24 h, 48 h and 72 h.

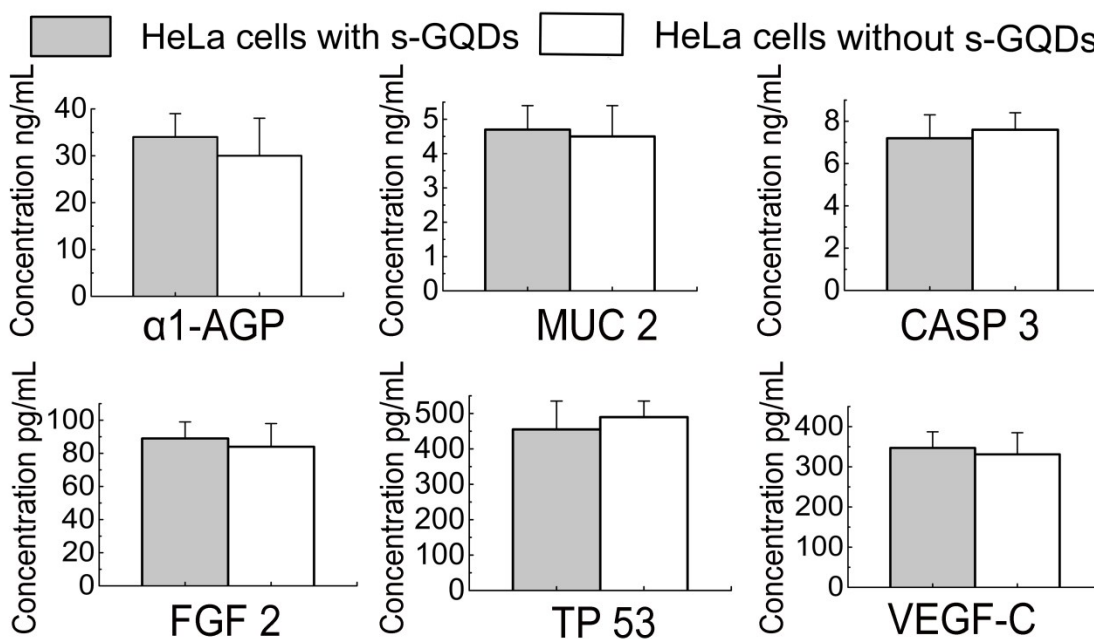


Figure 23 protein concentrations of HeLa cells incubated with or without s-GQDs. The concentrations are quantified by commercially available ELISAs. (α1-AGP: Alpha-1-Acid Glycoprotein; MUC 2: Mucin 2; VEGF-C: Vascular Endothelial Growth Factor C; FGF 2: Basic Fibroblast Growth Factor; TP53: Tumor Protein p53; CASP 3: Caspase 3). Error bars represent standard deviations from three replicate experiments.

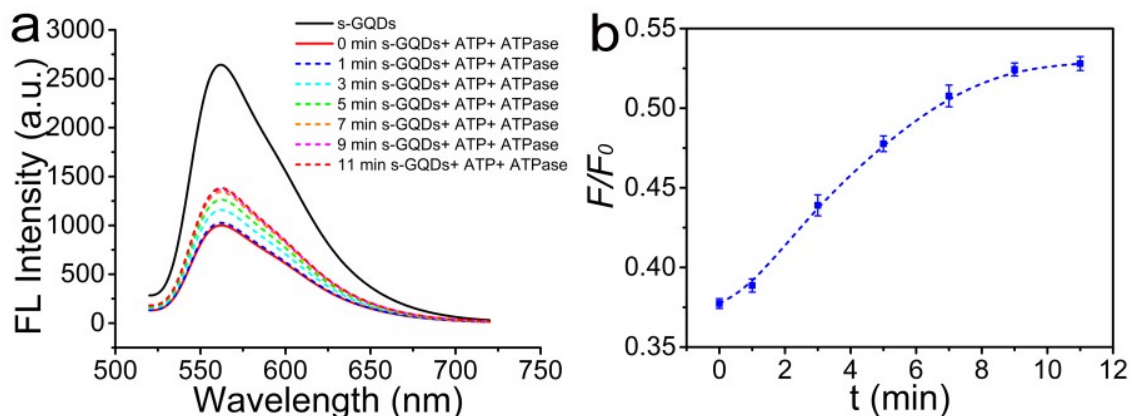


Figure S24 The fluorescence resuming ratio of s-GQD in presence of 4 μM ATP were evaluated by adding 40 μg ATPase at different time (0 min, 1min, 3 min, 5 min, 7 min and 11 min).

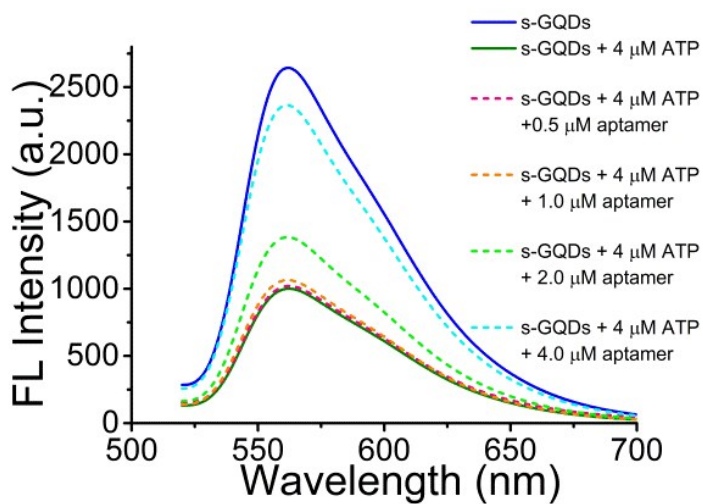


Figure S25 The fluorescence resuming ratio of s-GQD in presence of 4 μM ATP were evaluated by adding different concentration of ATP aptamer (0, 0.5, 1.0, 2.0 and 4.0 μM).

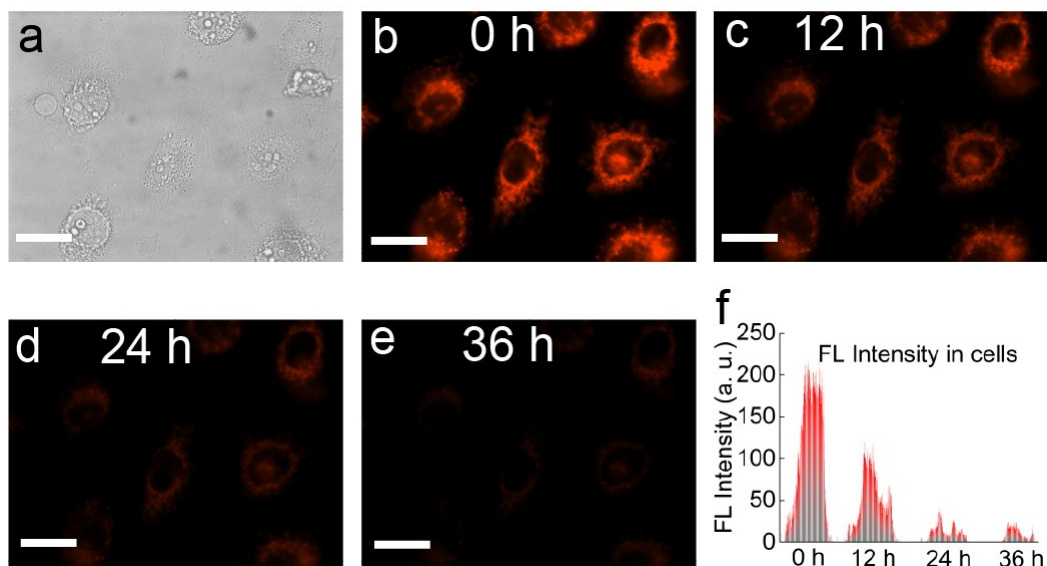


Figure S26 The excretion of s-GQDs out of cells. (a) Bright field image of HeLa cells. (b-e) Laser confocal microscopic images of s-GQDs in HeLa cells at different times after incubating with pure cell culture medium without s-GQDs. The cells were incubated with s-GQDs for 12 h before imaging. (f) Quantitative analysis of the fluorescence intensity of s-GQDs in HeLa cells at different times. The scale bar is 10 μm .

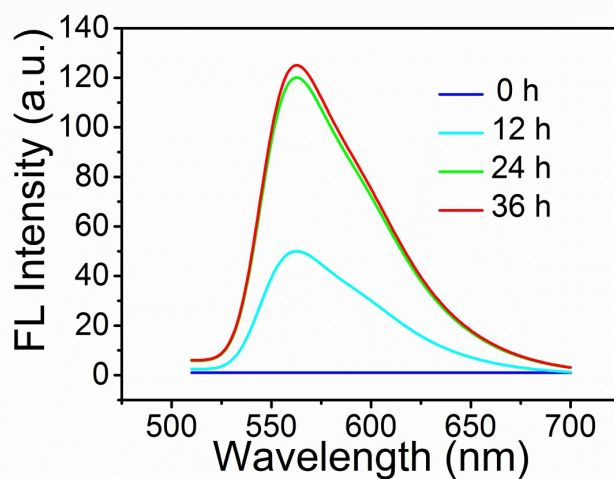


Figure S27 Fluorescence emission spectra of s-GQDs ($\lambda_{\text{ex}}=490$ nm) excreted from cells at different times. The cells were first incubated with s-GQDs for 12 h, and then incubating with pure cell culture medium without s-GQDs. We detected the fluorescence emission spectra of s-GQDs in the pure cell culture medium at different time. The increasing of the fluorescence intensity in the cell culture medium indicates that s-GQDs can be excreted from cells.

Notes:

To investigate whether s-GQDs could affect biochemistry processes, we did some experiments. First, the

long-term cell viability of HeLa cells has been assessed in 24 h, 48 h and 72 h. Second, we have quantified the amount of secreted proteins, glycoproteins and apoptosis proteins before and after the incubation of s-GQDs. Third, the bioactivity of ATP in s-GQDs solutions have been investigated using ATPase. Fourth, we monitored the removing of s-GQDs from cells.

First, HeLa cells were used to incubate with s-GQD for 24 h, 48 h and 72 h to evaluate the cytotoxicity of the s-GQD through the conventional Cell Counting Kit-8 (CCK-8) method. As shown in Figure S22, s-GQDs have no cytotoxicity when they are incubated with HeLa cells with a prolonged time.

Second, the amount of secreted proteins in living cells was quantified to evaluate whether cells are still functional after incubation of s-GQDs. The amount of secreted proteins, glycoproteins and apoptosis proteins were unchanged when the cells were treated with $100 \mu\text{g m L}^{-1}$ s-GQDs (Figure S23). Those results suggest that the HeLa cells are still functional when labeled with s-GQDs in the experimental concentration.

Third, the bioactivity of ATP in s-GQDs solutions have been investigated using ATPase (Figure S24). ATPase, a specific active enzyme of hydrolyzing ATP to phosphate and ADP, was used to simulate the process of intracellular ATP hydrolysis. In detail, $5 \mu\text{g mL}^{-1}$ s-GQD solution and $4 \mu\text{M}$ ATP were added, and then $40 \mu\text{g}$ ATPase were added for incubation (25°C , Tris-HCl pH 7.5). Afterwardes, the fluorescence intensity were measured to monitor the hydrolysis of ATP in present of ATPase at different time (from 0 min to 11 min). The results show an obvious fluorescence recovery in present of ATPase since ATP would be hydrolyzed to ADP in present of ATPase, and induced a weaker fluorescence quenching for s-GQD. Therefore, ATP can take part in biological response and the bioactivity of ATP would not be affected in presence of s-GQDs.

Fourth, we investigated the trap ability of the s-GQD to ATP. Briefly, $4 \mu\text{M}$ ATP was added into the s-GQD solution ($5 \mu\text{g mL}^{-1}$), and the fluorescence resuming ratio of s-GQD were evaluated by adding different concentration of ATP aptamer (0, 0.5, 1.0, 2.0 and $4.0 \mu\text{M}$). The fluorescence resuming ratio is proportional to the concentration of ATP aptamer (Figure S25). The results show that the binding between s-GQDs and ATP have a dynamic equilibrium and it would dissociate under certain conditions.

Finally, the s-GQDs can be excreted out of cells within 36 h after targeting the mitochondrion (Figure S26 and S27). The fluorescence of s-GQDs in mitochondrion would decrease after incubating with pure cell culture medium without s-GQDs. In contrast, the fluorescence of s-GQDs in cell culture increased gradually within the 36 h. The results indicate the s-GQDs can be excreted out of cells and the binding between s-GQDs and ATP has a dynamic equilibrium.

Taking together, the s-GQDs have no toxicity for cells for a prolonged time. The proteins would not be affected by s-GQDs. The trapped ATP can be hydrolyzed by enzyme and take part in essential

biochemistry processes. Meanwhile, the binding between s-GQDs and ATP has a dynamic equilibrium, and it would dissociate under certain conditions and excrete out of cells. We can draw the conclusion that s-GQDs would not affect biochemistry processes and are appropriate for in situ ATP imaging in live cells.

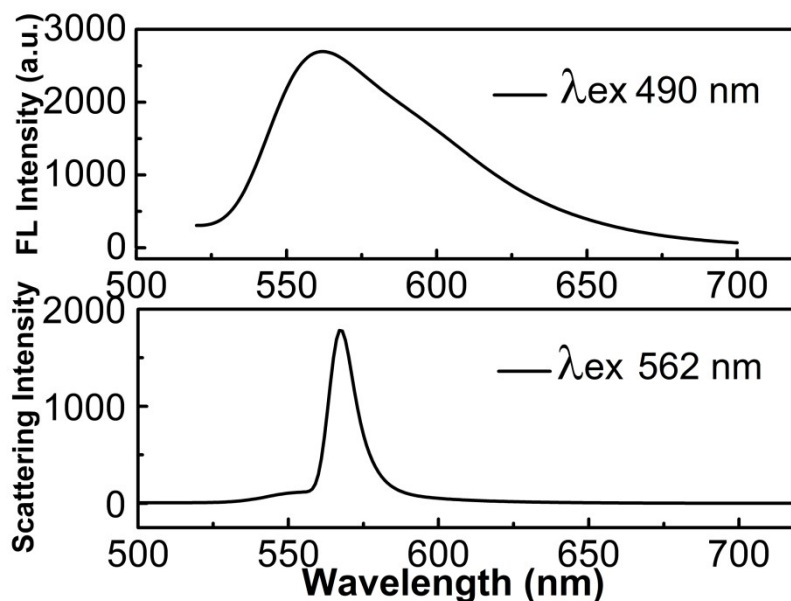


Figure S28 The fluorescence and scattering spectrum of s-GQDs when excitation wavelength at 490 nm and 562 nm, respectively (top: fluorescence spectrum; down: scattering spectrum).

Note: The s-GQDs would exhibit PL and the emission wavelength is 562 nm when excited with 490 nm, while the s-GQDs don't exhibit PL and only show a large scattering peak at 562 nm when excited with 562 nm.

Notes:

Chemically, we can predict or estimate the tendencies of various chemical processes according to the change of Gibbs free energy (ΔG). A chemical reaction will proceed spontaneously if the change of the total Gibbs free energy is negative. The ΔG is estimated according to the following equation:

$$\Delta G = \Delta H - T\Delta S$$

Where ΔH is the change of enthalpy. ΔS is the change of entropy.

In this paper, the π - π stacking and electrostatic interaction between ATP and s-GQDs are negative entropy process. This negative entropy change is not favor for a spontaneous chemical process. However, the π - π stacking and electrostatic interaction between ATP and s-GQDs are negative enthalpy process

which is favor for a spontaneous chemical process. Hence, the ΔG is needed to estimate the π - π stacking and electrostatic interaction between ATP and s-GQDs.

As the simplest prototype of π - π interactions, the ΔG is approximately equal to -10.2 KJ/mol when two benene molecules form a benzene dimer using a MP2/aug-cc-pVDZ method. Similar to the π - π interactions, the ΔG in electrostatic interaction between amino group on the edge of s-GQDs and triphosphate is approximately equal to -348.5 KJ/mol (calculated by Gaussian 09 program suite, B3LYP/6-31G).

Based on the negative ΔG in π - π stacking and electrostatic interaction, we may conclude that the dual recognition of ATP by s-GQDs is a spontaneous process.

References:

1. B. B. Chen, R. S. Li, M. L. Liu, H. Z. Zhang and C. Z. Huang, *Chem. Commun.*, 2017, **53**, 4958-4961.
2. B. Ju, H. Nie, Z. Liu, H. Xu, M. Li, C. Wu, H. Wang and S. X.-A. Zhang, *Nanoscale*, 2017, **9**, 13326-13333.
3. A. Kasprzak, M. Bystrzejewski, M. Koszytkowska-Stawinska and M. Popławska, *Green Chem.*, 2017, **19**, 3510-3514.
4. Z. Ding, F. Li, J. Wen, X. Wang and R. Sun, *Green Chem.*, 2018, **20**, 1383-1390.